JPSE (Journal of Physical Science and Engineering), Vol. 9, No. 2, 2024, Page 73–79.
DOI: 10.17977/um024v9i22024p73-79

JPSE
(Journal of Physical Science and Engineering)

http://journal2.um.ac.id/index.php/jpse
EISSN: 2541-2485

# The Role of CTAB Surfactant Composition on the Structural and Magnetic Properties of $Mn_{0.5}Zn_{0.5}Fe_2O_4$ Ferrofluid for Energy Harvesting Devices

**Received**
1 September 2024

**Revised**
29 September 2024

**Accepted for Publication**
20 October 2024

**Published**
31 October 2024

**Wa Ode Umratul Khazanah, Arif Hidayat*, Ahmad Taufiq, ST. Ulfawanti Intan Subadra**

Department of Physics, Faculty of Mathematics and Natural Sciences, Universitas Negeri Malang, Malang 65145, Indonesia.

*Corresponding Author's Email: arif.hidayat.fmipa@um.ac.id



**Abstract**

Concerns about environmental damage caused by pollution and the use of non-renewable energy sources have driven many researchers to explore sustainable energy-harvesting materials. This study successfully developed an energy harvester based on $Mn_{0.5}Zn_{0.5}Fe_2O_4$ ferrofluid. Notably, Cetyl Trimethyl Ammonium Bromide (CTAB) was used as the surfactant in the synthesis of the $Mn_{0.5}Zn_{0.5}Fe_2O_4$ ferrofluid via the coprecipitation method. The CTAB mass was varied at 0, 0.25, 0.5, 0.75, and 1 gram, labeled as MZC0, MZC0.25, MZC0.5, MZC0.75, and MZC1. XRD patterns showed that MZC0 have a cubic spinel structure, while CTAB addition altered the structure to monoclinic, following CTAB's pattern. FTIR spectra at 418.1, 571.1, and 445.3 $cm^{-1}$ confirmed Mn–O, Fe–O, and Zn–O stretching, indicating successful spinel formation. Meanwhile, FTIR bands at 2800 and 2900 $cm^{-1}$ in MZC0.25–MZC1 samples were due to C–H stretching from CTAB. VSM analysis revealed a decreasing saturation magnetization (Ms) with increasing CTAB. SEM images confirmed surfactant coating on nanoparticles. Energy harvesting tests showed output voltages of -0.4 to 2.9 V and low induced currents (0.3–1.9 μA), suggesting the potential of $Mn_{0.5}Zn_{0.5}Fe_2O_4$/CTAB-based ferrofluid as an eco-friendly energy harvester.

**Keywords:** Ferrofluid, $Mn_{0.5}Zn_{0.5}Fe_2O_4$, CTAB, Energy Harvesting.

## 1. Introduction

In recent years, global warming has emerged as a critical global concern demanding immediate scientific and policy-oriented attention. [1]. The rise in the Earth's average temperature caused by greenhouse gas emissions has led to climate change that significantly affects the environment. Pollution resulting from the combustion of fossil fuels has greatly contributed to carbon dioxide ($CO_2$) emissions, which is one of the main causes of climate change and global warming [2][3][4]. Therefore, efforts are needed to reduce dependence on fossil energy sources by developing more environmentally friendly alternative energy. Consequently, extensive research efforts have been directed toward energy harvesting technologies as a promising solution. Energy harvesting refers to the process of capturing and converting otherwise lost energy into usable electrical power. [5]. One type of energy harvester currently being developed by many researchers is mechanical energy harvesting derived from ferrofluid vibrations. These vibrations can be harvested into electrical energy using the electromagnetic force effect based on Faraday's law of induction [6]. The change in induction caused by ferrofluid vibrations inside the coil generates magnetic field fluctuations around the coil that trigger the emergence of an electromotive force (EMF), which can be utilized as an alternative energy source.

Ferrofluid or magnetic fluid is a heterogeneous mixture between liquid and solid phases [7]. Ferrofluid consists of three components: magnetic compounds ($Fe_3O_4$) in nano-size, surfactants that coat the magnetic material, and a carrier liquid that suspends the magnetic material to distribute it evenly throughout the fluid [8]. Surfactants in ferrofluids serve to enhance particle dispersion, thereby

stabilizing the magnetic material in the liquid suspension [9]. This stability greatly affects the performance of ferrofluid in energy harvesting applications. A comprehensive study on the development of ferrofluid as an energy harvester has been conducted. Hannon et al., 2023 developed a ferrofluid-based energy harvester using $Fe_3O_4$ as the main material with water as the surfactant [5]. The result showed a relatively high voltage output of 1.1 mV. Chen, 2023 synthesized water-based $Fe_3O_4$ ferrofluid using anionic surfactants and obtained a maximum current value of 1.05 nA [10]. Santi, 2023 synthesized $Mn_{0.5}Zn_{0.5}Fe_2O_4$ using TMAH-based surfactants and obtained a relatively small induced current of 136.36 μA [11]. However, to the best of the authors' knowledge, no prior studies have specifically investigated specifically exploring the use of CTAB surfactant in the synthesis of ferrofluids. Notably, CTAB exhibits the capability to form a more stable and homogeneous layer on the surface of nanoparticles, which potentially enhances dispersion stability and influences the magnetic and electromagnetic response properties of ferrofluids [12].

Cetyltrimethylammonium bromide (CTAB) is a cationic surfactant that has a significant effect on the stabilization and properties of nanoparticles, particularly in applications involving ferrofluids. The interaction of CTAB with nanoparticles leads to the formation of a stable and uniform coating on their surface, improving dispersion stability [12]. The ability of CTAB to prevent agglomeration is related to its role in forming a protective layer around the particles, thereby reducing the magnetic dipole-dipole attraction that commonly causes clumping [13]. In ferrofluids, this stability is crucial because it affects the magnetic properties and electromagnetic response, which ultimately influence the effectiveness of ferrofluid performance as an energy harvester. Nevertheless, the use of CTAB surfactants must be carefully controlled, as excessive surfactant concentration can negatively affect the characteristics of ferrofluids. The concentration of CTAB may influence characteristics such as saturation magnetization and magnetic susceptibility of ferrofluids, both of which are important parameters in energy harvester applications that utilize electromagnetic effects [14].

In light of the preceding discussion, this research is intended to conduct an in-depth investigation into the influence of CTAB surfactant composition variations on the structural and magnetic characteristics of $Mn_{0.5}Zn_{0.5}Fe_2O_4$-based ferrofluids for energy harvesting applications.

## 2. Methods

### *2.1. Materials*

This study used iron sand, hydrochloric acid (HCl) solution, manganese chloride ($MnCl_2$), zinc chloride ($ZnCl_2$), ammonia solution ($NH_4OH$), and the surfactant CTAB as base materials to synthesize $Mn_{0.5}Zn_{0.5}Fe_2O_4$ ferrofluid.

### *2.2. Synthesis of $Mn_{0.5}Zn_{0.5}Fe_2O_4$ Ferrofluid*

The synthesis was carried out using the coprecipitation method in two steps: the synthesis of $Mn_{0.5}Zn_{0.5}Fe_2O_4$ nanoparticles and the preparation of $Mn_{0.5}Zn_{0.5}Fe_2O_4$ ferrofluid. In the nanoparticle synthesis step, 20 grams of iron sand were reacted with 58 mL of HCl to obtain an $FeCl_3$ solution. This solution was then reacted with $MnCl_2$ and $ZnCl_2$, followed by titration using $NH_4OH$ solution to facilitate precipitation. For the ferrofluid preparation steps, 1 gram of $Mn_{0.5}Zn_{0.5}Fe_2O_4$ nanoparticles was dispersed in 5 mL of distilled water and mixed with CTAB surfactant. The mixture was stirred for 30 minutes to ensure homogeneity and interaction between the surfactant and nanoparticle surface.

### *2.3. Characterization Techniques*

A series of characterizations were conducted to gain further understanding of the properties of the ferrofluid:

a) X-ray Diffraction (XRD) was used to analyze the crystalline structure formed in the sample.
b) Fourier-transform Infrared Spectroscopy (FTIR) was employed to identify the functional groups contained in the sample and to evaluate the crystalline phase and structure.

c) Scanning Electron Microscopy (SEM) was used to observe the morphology and determine particle size distribution.
d) Vibrating Sample Magnetometer (VSM) was used to investigate the magnetic behavior of the sample.
e) Current-voltage (IV) testing was performed to assess the energy harvesting potential of the synthesized ferrofluid.

## 3. Results and Discussion

The MZC0 sample exhibits a diffraction pattern similar to that of the MZ sample. This pattern shows good agreement with the crystal planes (220), (311), (400), (422), (511), and (440), which were detected at 2θ angles of 30.2°, 35.4°, 43°, 53.3°, 56.9°, and 62.5°, respectively. Among these planes, the highest intensity peak was observed at a 2θ angle of 35.5°. This pattern corresponds to the characteristic diffraction pattern of magnetite, which possesses a cubic spinel crystal structure and belongs to the Fd-3m space group. These findings are consistent with those reported by R. Müller (2006), who stated that ferrite-based ferrofluid samples using water as a surfactant and carrier liquid exhibit a diffraction pattern similar to that of $Fe_3O_4$ magnetite [15]. The addition of CTAB to the $Mn_{0.5}Zn_{0.5}Fe_2O_4$ ferrofluid induced a change in its crystal structure. The original cubic spinel phase was transformed into a monoclinic structure following the incorporation of CTAB, which is consistent with the standard crystal structure of CTAB. This structural transformation is indicated by the emergence of new diffraction peaks at 2θ angles of 21°, 24°, and 28°, corresponding to the (002), (102), and (210) planes of a monoclinic structure (COD 96-720-6058). These results suggest that CTAB not only acts as a surfactant but also interacts with the particle surface and alters the crystal arrangement. The observed changes in crystal structure may also be attributed to the fact that XRD primarily detects atoms located on the surface of the particles. In ferrofluids, the surface of $Mn_{0.5}Zn_{0.5}Fe_2O_4$ particles is coated with a surfactant layer, resulting in diffraction patterns that predominantly originate from CTAB molecules. Similar findings were reported by R. E. Saputro (2019), who explained that the diffraction pattern of dried ferrofluid samples tends to reflect the surfactant rather than the core material [16]. In this case, the sample surface is dominated by the CTAB surfactant rather than the $Mn_{0.5}Zn_{0.5}Fe_2O_4$ core.

The intensity of the diffraction peaks increases with the increasing mass of CTAB surfactant used. The diffraction peak intensities at the highest peak for the MZC0.25, MZC0.5 and MZC0.75 samples are 448 a.u., 775 a.u. and 1167 a.u. This indicates that the addition of CTAB contributes to an enhancement in crystallinity or the amount of crystalline phase in the samples, as reflected by the increased diffraction peak intensity [17]

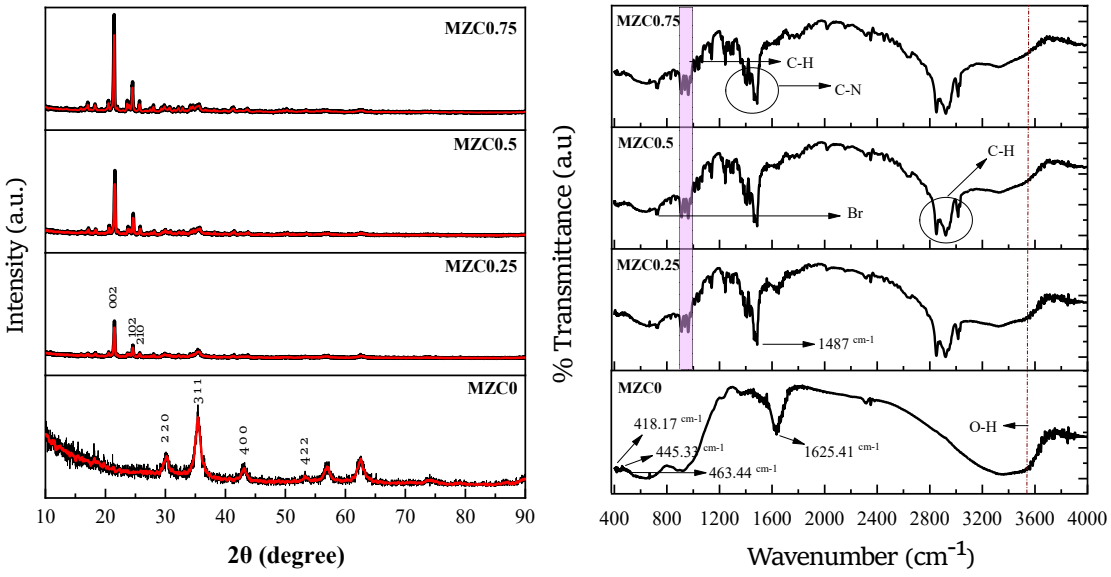


**Figure 1.** XRD Diffraction Patterns (a) and The FTIR Spectra (b) of the $Mn_{0.5}Zn_{0.5}Fe_2O_4$ Ferrofluid.

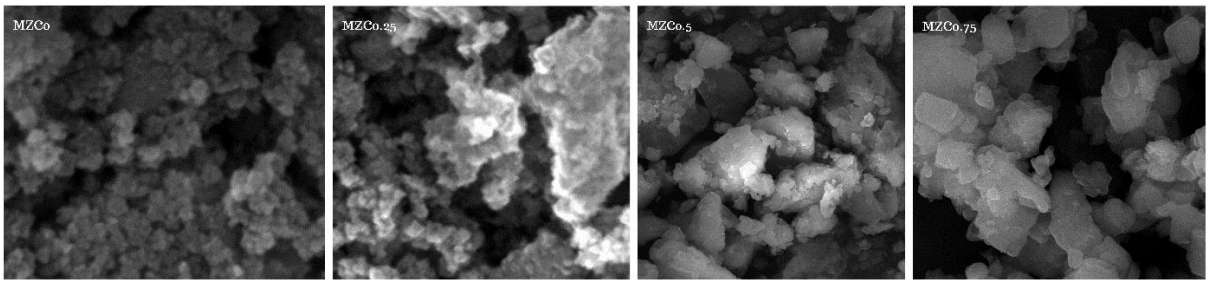


**Figure 2.** The Morphology of the $Mn_{0.5}Zn_{0.5}Fe_2O_4$ Ferrofluid.

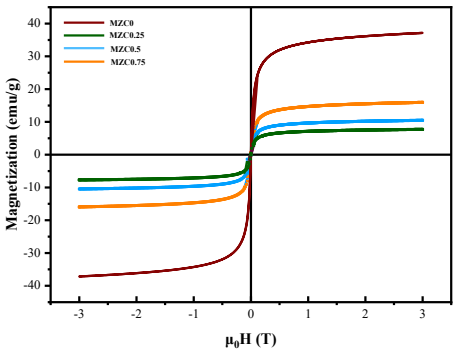


**Figure 3.** Magnetization Curve of $Mn_{0.5}Zn_{0.5}Fe_2O_4$ Ferrofluid.

In MZC0, the FTIR spectrum at the wavenumber of 418.2 $cm^{-1}$ is associated with Mn–O bonding, 445.3 $cm^{-1}$ corresponds to Zn–O bonding, and 463.4 $cm^{-1}$ is attributed to Fe–O bonding at the octahedral (B) site. Meanwhile, the peak at 571 $cm^{-1}$ is related to the stretching vibration of the Fe–O bond at the octahedral (B) site [18]. The bending vibration in the FTIR spectrum at the wavenumber of 1625.4 $cm^{-1}$ is associated with the hydroxyl (O–H) group of water molecules [19], and the peak at 3392.35 $cm^{-1}$ corresponds to the stretching vibration of the O–H bond [20]. The addition of CTAB surfactant to the $Mn_{0.5}Zn_{0.5}Fe_2O_4$ ferrofluid significantly influenced the resulting FTIR spectrum. This alteration is indicated by the emergence of new peaks in the FTIR spectrum, which are associated with the functional groups of CTAB interacting with the surface of the $Mn_{0.5}Zn_{0.5}Fe_2O_4$ material. Intense absorption bands detected in the wavenumber range of 2841–2900 $cm^{-1}$ are attributed to the stretching vibrations of methyl (C–H) groups in CTAB molecules [10]. Additionally, the absorption bands in the range of 904.68–975 $cm^{-1}$ are associated with out-of-plane bending vibrations of methyl ($CH_3$) groups. Another absorption band appearing in the range of 1400–1497 $cm^{-1}$ corresponds to C–N bonding, while the absorption band at 725 $cm^{-1}$ is linked to the presence of bromide ($Br^-$) ions from CTAB [21].

The morphology of the $Mn_{0.5}Zn_{0.5}Fe_2O_4$ ferrofluid samples is shown in Figure 2. It can be observed that the MZC0 sample exhibits a more aggregated structure with smaller and denser particles. Furthermore, the samples MZC0.25 to MZC0.75 begin to show the growth of larger particles with a more granular and rough morphology, as well as partial agglomeration, while still maintaining nanoscale dimensions as the mass of CTAB surfactant increases. Increasing the amount of surfactant can lead to a thicker adsorbed layer on the magnetic nanoparticles. This augmented bilayer, in turn, increases the effective hydrodynamic diameter of the particles or aggregates, which manifests as a larger morphology [22]. In particular, Widiyandari et al. (2008) investigated surfactant-excess conditions in non-polar ferrofluids and observed that free surfactant molecules contribute to forming a more extended interparticle barrier, thereby leading to a larger effective size of the dispersed entities.

Figure 3 shows the hysteresis curve of the $Mn_{0.5}Zn_{0.5}Fe_2O_4$/CTAB ferrofluid sample. Based on the figure, it can be seen that all samples exhibit superparamagnetic behavior, characterized by an S-shaped curve without a hysteresis loop [23]. The MZC0 sample has a saturation magnetization (Ms) value of 36.4 emu/g, which then decreases drastically upon the addition of the CTAB surfactant. The addition of CTAB causes a significant reduction in the Ms value. The MZC0.25 sample has an Ms value of 6.73 emu/g. In the MZC0.5 and MZC0.75 samples, the Ms value increases again to 9.18 emu/g and

13.97 emu/g, respectively. Saturation magnetization is a state in which all magnetic moments in the system are aligned with the direction of the magnetic field under the application of a very strong magnetic field [20]. On the other hand, CTAB is not a magnetic material. It is an organic surfactant and does not contain any metallic elements, so it cannot produce magnetic moments [24]. This leads to a drastic decrease in the Ms value upon the addition of CTAB. In addition, environmental conditions and the synthesis method used can also affect the magnetic properties of a material [25]. Magnetic properties of $Mn_{0.5}Zn_{0.5}Fe_2O_4$ ferrofluid are shown in Table 1.

**Tabel 1.** The Magnetic Properties of $Mn_{0.5}Zn_{0.5}Fe_2O_4$ Ferrofluid.

| Sampel | Ms (emu/g) | Mr (emu/g) | Hc (T) | χ |
|---|---|---|---|---|
| MZC0 | 36.4 | 0.009 | 0.008 | 1.475 |
| MZC0.25 | 6.7 | 0.002 | 0.003 | 0.269 |
| MZC0.5 | 9.2 | 0.003 | 0.001 | 0.333 |
| MZC0.75 | 13.97 | 0.004 | 0.001 | 0.001 |

The voltage values are relatively high, ranging from -0.4 to 2.9 V. As a result, the induced current values produced are relatively low, ranging from 0.3 to 1.9 μA. The addition of CTAB surfactant composition to $Mn_{0.5}Zn_{0.5}Fe_2O_4$ ferrofluid results in fluctuating current and voltage values. The appropriate surfactant mass concentration in the ferrofluid plays a role in controlling the crystallinity and particle size, thereby optimizing the saturation magnetization value. Uniformly sized crystals can enhance the interaction between particles and the external magnetic field, where this interaction plays an important role in the electromagnetic induction effect for generating voltage and induced current.

In addition, the increased composition of CTAB surfactant shows larger particle sizes. The greater the amount of surfactant added, the thicker the surfactant layer coating the $Mn_{0.5}Zn_{0.5}Fe_2O_4$ nanomaterial becomes. This weakens the magnetic interaction between particles, resulting in a smaller induced current. The excessive addition of surfactant leads to the formation of a thicker nanomagnetic layer on the $Mn_{0.5}Zn_{0.5}Fe_2O_4$ nanomaterial, which increases the separation of magnetic cores. The increased distance between particles reduces dipolar magnetic interactions, as magnetic coupling is highly sensitive to the inter-particle distance. Consequently, the effective magnetization and the induced current generated under the applied magnetic field decrease. The thicker surfactant layer effectively acts as a barrier that isolates the nanoparticles and introduces magnetically disordered interfacial regions [26][27].

## 4. Conclusion

The addition of CTAB surfactant to $Mn_{0.5}Zn_{0.5}Fe_2O_4$ ferrofluid significantly influences its crystal structure, morphology, and magnetic properties. XRD analysis indicates a transition from a cubic spinel to a monoclinic structure and an increase in crystallinity with higher CTAB mass. FTIR results confirm the interaction between CTAB functional groups and the nanoparticle surface. Morphologically, increased CTAB leads to larger particles and thicker surfactant layers, which affect interparticle interactions. Magnetic characterization shows a superparamagnetic nature across all samples, with saturation magnetization (Ms) decreasing significantly after CTAB addition due to reduced magnetic coupling. However, Ms increases slightly with further CTAB content as crystallinity improves. The voltage output remains high, but the induced current declines due to weakened dipolar interactions from increased particle separation. Overall, CTAB plays a dual role as a stabilizing agent and a structural modifier, with excessive amounts potentially reducing magnetic and energy-harvesting efficiency. Thus, optimizing CTAB concentration is essential for improved performance.

**Acknowledgment**
This research was supported by Universitas Negeri Malang through the PNBP thesis grant scheme awarded to Prof. Dr. Arif Hidayat, M.Si. in 2024.

**References**


[1] A. Jorgenson, W. Longhofer, and D. Grant, "Disproportionality in Power Plants' Carbon Emissions: A Cross-National Study," *Sci. Rep.*, vol. 6, no. April, pp. 1–7, 2016, doi: 10.1038/srep28661.

[2] L. Hauchhum and P. Mahanta, "$CO_2$ Capture onto Zeolite 13X and Zeolite 4A by Pressure Swing Adsorption in a Fixed Bed," *Appl. Mech. Mater.*, vol. 592–594, pp. 1456–1460, Jul. 2014, doi: 10.4028/www.scientific.net/AMM.592-594.1456.

[3] D. Kunda and H. Phiri, "An Approach for Predicting $CO_2$ Emissions using Data Mining Techniques," *Int. J. Comput. Appl.*, vol. 172, no. 3, pp. 7–10, 2017, doi: 10.5120/ijca2017915098.

[4] M. Ansaripour, M. Haghshenasfard, and A. Moheb, "Experimental and Numerical Investigation of CO 2 Absorption Using Nanofluids in a Hollow-Fiber Membrane Contactor," *Chem. Eng. Technol.*, vol. 41, no. 2, pp. 367–378, Feb. 2018, doi: 10.1002/ceat.201700182.

[5] N. Hannon, C. W. Harrison, M. J. Kraśny, and D. Zabek, "Liquid Vibration Energy Harvesting Device Using Ferrofluids," *Micromachines*, vol. 14, no. 8, p. 1588, Aug. 2023, doi: 10.3390/mi14081588.

[6] S. P. Beeby and T. O'Donnell, "Electromagnetic Energy Harvesting," in *Energy Harvesting Technologies*, Boston, MA: Springer US, pp. 129–161. doi: 10.1007/978-0-387-76464-1_5.

[7] W. Yang, Y. Zhang, X. Yang, C. Sun, and Y. Chen, *Systematic analysis of ferrofluid: a visualization review, advances engineering applications, and challenges*, vol. 24, no. 6. Springer Netherlands, 2022. doi: 10.1007/s11051-022-05477-5.

[8] O. Oehlsen, S. I. Cervantes-Ramírez, P. Cervantes-Avilés, and I. A. Medina-Velo, "Approaches on Ferrofluid Synthesis and Applications: Current Status and Future Perspectives," *ACS Omega*, vol. 7, no. 4, pp. 3134–3150, 2022, doi: 10.1021/acsomega.1c05631.

[9] A. Shankar, M. Chand, G. A. Basheed, S. Thakur, and R. P. Pant, "Low temperature FMR investigations on double surfactant water based ferrofluid," *J. Magn. Magn. Mater.*, vol. 374, pp. 696–702, 2015, doi: 10.1016/j.jmmm.2014.09.038.

[10] G. Quan *et al.*, "Lactosaminated mesoporous silica nanoparticles for asialoglycoprotein receptor targeted anticancer drug delivery," *J. Nanobiotechnology*, vol. 13, no. 1, pp. 1–12, 2015, doi: 10.1186/s12951-015-0068-6.

[11] D. Santi, S. Zuhroh, A. Hidayat, S. T. U. Intan Subadra, and A. Taufiq, "Ferrofluid $Mn_{0.5}Zn_{0.5}Fe_2O_4$ as Harvesting Energy: Preliminary Study," *Key Eng. Mater.*, vol. 950, pp. 39–40, 2023, doi: 10.4028/p-ChTj63.

[12] A. Shokuhfar and S. S. Seyyed Afghahi, "The heating effect of iron-cobalt magnetic nanofluids in an alternating magnetic field: application in magnetic hyperthermia treatment," *Nanoscale Res. Lett.*, vol. 8, no. 1, p. 540, Dec. 2013, doi: 10.1186/1556-276X-8-540.

[13] X. Yang *et al.*, "Photothermal and adsorption effects of silver selenide nanoparticles modified by different surfactants in nursing care of cancer patients," *Sci. Technol. Adv. Mater.*, vol. 21, no. 1, pp. 584–592, Jan. 2020, doi: 10.1080/14686996.2020.1800367.

[14] R. Y. Hong, S. Z. Zhang, Y. P. Han, H. Z. Li, J. Ding, and Y. Zheng, "Preparation, characterization and application of bilayer surfactant-stabilized ferrofluids," *Powder Technol.*, vol. 170, no. 1, pp. 1–11, Nov. 2006, doi: 10.1016/j.powtec.2006.08.017.

[15] R. Müller, R. Hergt, S. Dutz, M. Zeisberger, and W. Gawalek, "Nanocrystalline iron oxide and Ba ferrite particles in the superparamagnetism-ferromagnetism transition range with ferrofluid applications," *J. Phys. Condens. Matter*, vol. 18, no. 38, 2006, doi: 10.1088/0953-8984/18/38/S01.

[16] R. E. Saputro, A. Taufiq, N. Hidayat, Sunaryono, Y. A. Hariyanto, and A. Hidayat, "Preparation of $Fe_3O_4$/OA/DMSO Ferrofluids using a Double Surfactant System as Antifungal Materials Candidate," *IOP Conf. Ser. Mater. Sci. Eng.*, vol. 515, no. 1, 2019, doi: 10.1088/1757-899X/515/1/012029.

[17] M. Deepty, C. Srinivas, E. R. Kumar, N. K. Mohan, and C. L. Prajapat, "XRD , EDX , FTIR and ESR spectroscopic studies of co-precipitated Mn – substituted Zn – ferrite nanoparticles Short communication XRD , EDX , FTIR and ESR spectroscopic studies of co-precipitated Mn – substituted Zn – ferrite nanoparticles," *Ceram. Int.*, vol. 45, no. 6, pp. 8037–8044, 2019, [Online]. Available: https://doi.org/10.1016/j.ceramint.2019.01.029

[18] N. H. Abdullah, M. S. Mustaffa, M. N. Hamidon, F. N. Shafie, I. Ismail, and I. R. Ibrahim, "Isochronal recovery behaviour on electromagnetic properties of polycrystalline nickel zinc ferrite ($Ni_{0.5}Zn_{0.5}Fe_2O_4$) prepared via mechanical alloying," *Sci. Rep.*, vol. 11, no. 1, pp. 1–11, 2021, doi: 10.1038/s41598-021-99236-6.

[19] S. Bahtiar *et al.*, "Synthesis, Investigation on Structural and Magnetic Behaviors of Spinel M-Ferrite [M = Fe; Zn; Mn] Nanoparticles from Iron Sand," *IOP Conf. Ser. Mater. Sci. Eng.*, vol. 202, no. 1, 2017, doi: 10.1088/1757-899X/202/1/012052.

[20] S. F. Aval, A. Akbarzadeh, M. R. Yamchi, F. Zarghami, K. Nejati-Koshki, and N. Zarghami, "Gene silencing effect of SiRNA-magnetic modified with biodegradable copolymer nanoparticles on hTERT gene expression in lung cancer cell line," *Artif. Cells, Nanomedicine Biotechnol.*, vol. 44, no. 1, pp. 188–193, 2016, doi: 10.3109/21691401.2014.934456.

[21] S. A. Elfeky, S. E. Mahmoud, and A. F. Youssef, "Applications of CTAB modified magnetic nanoparticles for removal of chromium (VI) from contaminated water," *J. Adv. Res.*, vol. 8, no. 4, pp. 435–443, 2017, doi: 10.1016/j.jare.2017.06.002.

[22] H. Widiyandari, F. Iskandar, N. Hagura, and K. Okuyama, "Preparation and characterization of nanopigment-poly(styrene- co - n -butyl acrylate- co -methacrylic acid) composite particles by high speed homogenization-assisted suspension polymerization," *J. Appl. Polym. Sci.*, vol. 108, no. 2, pp. 1288–1297, Apr. 2008, doi: 10.1002/app.27814.

[23] C. Wang, Y. Wang, Y. Cheng, W. Huang, B. Zou, and X. Cao, "Effects of surfactants on the structure and crystal growth behavior of Sm 2Zr 2O 7 nanocrystalline," *Powder Technol.*, vol. 225, pp. 130–135, 2012, doi: 10.1016/j.powtec.2012.03.050.

[24] T. Wu *et al.*, "A comprehensive study on MnZn ferrite materials with high saturation magnetic induction intensity and high permeability for magnetic field energy harvesting," *J. Magn. Magn. Mater.*, vol. 590, no. October 2023, p. 171635, 2024, doi: 10.1016/j.jmmm.2023.171635.

[25] S. Khashan, S. Dagher, N. Tit, A. Alazzam, and I. Obaidat, "Novel method for synthesis of $Fe_3O_4$@$TiO_2$ core/shell nanoparticles," *Surf. Coatings Technol.*, vol. 322, no. August, pp. 92–98, 2017, doi: 10.1016/j.surfcoat.2017.05.045.

[26] Y. Yuan, D. Rende, C. L. Altan, S. Bucak, R. Ozisik, and D.-A. Borca-Tasciuc, "Effect of Surface Modification on Magnetization of Iron Oxide Nanoparticle Colloids," *Langmuir*, vol. 28, no. 36, pp. 13051–13059, Sep. 2012, doi: 10.1021/la3022479.

[27] Y. Köseoğlu, F. Yıldız, D. K. Kim, M. Muhammed, and B. Aktaş, "EPR studies on Na-oleate coated Fe 3 O 4 nanoparticles," *Phys. status solidi*, vol. 1, no. 12, pp. 3511–3515, Dec. 2004, doi: 10.1002/pssc.200405493.